Microwave induced nonlocal transport in two-dimensional electron system.

A. D. Levin,[1] Z. S. Momtaz, [1] G. M. Gusev,[1] and A. K. Bakarov, [2]
[1] *Instituto de Física da Universidade de São Paulo, 135960-170, São Paulo, SP, Brazil and*
[2] *Institute of Semiconductor Physics, Novosibirsk 630090, Russia*
(Dated: April 23, 2014)

We observe microwave induced nonlocal resistance in magnetotransport in single and bilayer electronic systems. The obtained results provide evidence for an edge state current stabilized by microwave irradiation due to nonlinear resonances. Our observation are closely related to microwave induced oscillations and zero resistance states in a two-dimensional (2D) electron system.

arXiv:1404.5295v1 [cond-mat.mes-hall] 22 Apr 2014

A few years ago, a new class of the non-equilibrium phenomena was observed, when an ultrahigh mobility 2D electron gas, subjected to a weak magnetic field was also irradiated with microwaves [1]. This included microwave-induced resistance oscillations (MIROs) [2] and a zero-resistance state (ZRS)[3]. Many microscopic mechanisms of MIRO have been proposed, mainly originating from the scattering-assisted electron transitions between different Landau levels in the presence of microwave excitation. The most developed theories account for spatial displacement of electrons along the applied dc field under scattering-assisted microwave absorption ("displacement" mechanism) [4, 5], and an oscillatory contribution to the isotropic part of the electron distribution function ("inelastic" mechanism) [6]. Both these mechanisms describe the periodicity and phase of MIROs observed in experiments and can lead to an absolute negative conductivity $\sigma < 0$. ZRS emerges from the instability of a homogeneous state with $\sigma < 0$ and the nonequilibrium phase transition into a domain state with zero net resistance [22]. Two more alternative approaches to the MW-induced effects in dissipative resistance, such as the radiation-driven electron-orbit [8] and near-contact region [9] models, have been recently proposed.

A striking similarity has been emphasized between QHE and ZRS: both effects exhibit vanishing longitudinal resistance R_{xx}, when the propagation along the sample edge is ballistic, although the magnetic field intensity is quite different. One naturally expects that a strong magnetic field stabilizes edge states, and, therefore, that the QHE is robust against disorder [10]. It has been shown that microwave radiation can also stabilize guiding along sample edges in the presence of a relatively weak magnetic field leading to a ballistic dissipation-less transport regime, which also results in vanishing R_{xx} [11]. Indeed such transport is much less robust than those in the QHE regime and requires samples with ultrahigh electron mobility. This model also avoids the fundamental assumption made in those approaches [4–6] that cyclotron harmonic absorption at high j can be explained by the presence of the short range potential, while in high mobility samples the long range potential plays a dominant role.

The method used for probing the property of the edge states is nonlocal electrical measurement. If a finite voltage is applied between a pair of the probes, a net current appears along the sample edge, which can be detected by another pair of voltage probes far away from the bulk current path.

In this letter we present studies of the nonlocal resistance in narrow (NQW) and wide (WQW) quantum wells, which represent single and two-subband 2D systems respectively, exposed to microwave irradiation. We find a relatively large ($\sim 0.05 \times R_{xx}$) nonlocal resistance in the vicinity of the ratio $j \approx \omega/\omega_c \approx 3.15/4$, where ω is the radiation angular frequency, $\omega_c = eB/m$ is the cyclotron angular frequency, and m is the effective mass of the electrons. We attribute the observed nonlocality to the existence of edge states stabilized by microwave irradiation and a weak magnetic field. We provide a model taking into account the edge and bulk contributions to the total current in the local and nonlocal geometries.

We have studied both narrow (14 nm) and wide (45 nm) quantum wells with an electron density of $n_s \simeq 1.0 \times 10^{12}$ cm^{-2} and a mobility of $\mu \simeq 1.7 - 3.2 \times 10^6$ cm^2/V s, respectively, at temperature of 1.4 K and after a brief illumination with a red diode. Owing to charge redistribution, WQWs with high electron density form a bilayer configuration, i.e. two wells near the interfaces are separated by an electrostatic potential barrier and two subbands appear as a result of tunnel hybridization of 2D electron states (symmetric and antisymmetric), which are separated in energy by Δ_{SAS}. In NQW electrons also occupy two subbands after illumination, but the carrier density of the second subband is much smaller than the density of the lower subband. We have measured resistance on two different types of the devices. Device A is a conventional Hall bar patterned structure (length l × width w=500 μm×200 μm) with six contacts for identifying nonlocal transport over macroscopic distances. Device B is designed for multi-terminal measurements. The sample consists of three $5\mu m$ wide consecutive segments of different length $(5, 15, 5\mu m)$, and 8 voltage probes [12]. The measurements have been carried out in a VTI cryostat with a waveguide to deliver MW irradiation (frequency range 110 to 170 GHz) down to the sample and by using a conventional lock-in technique to measure the longitudinal resistance R_{xx}. In WQW the

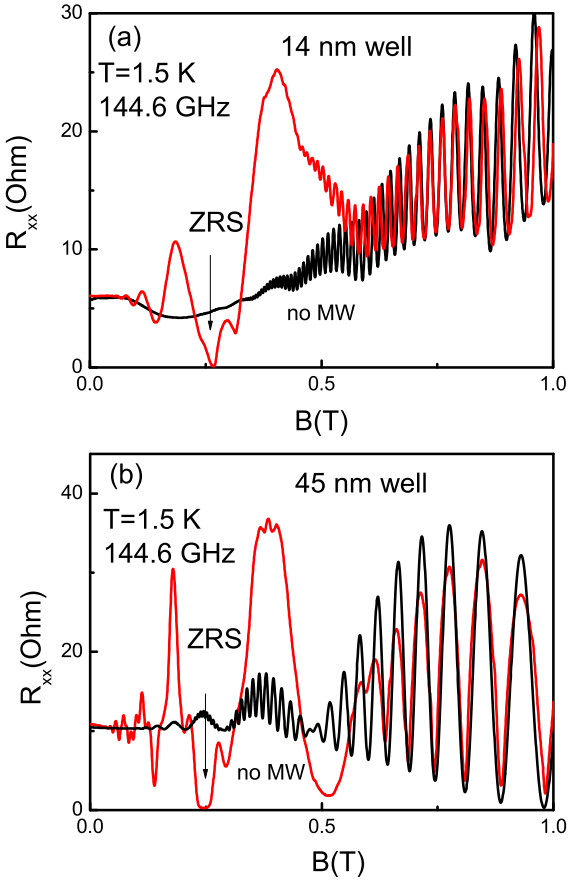

FIG. 1: (Color online) Longitudinal R_{xx} (I=1,4; V=2,3) resistance without (no MW) and with microwave irradiation (144,6 GHz) in (a) a narrow (14 nm) and a (b) wide (45 nm) quantum well. Arrows indicate the regions of vanishing resistance.

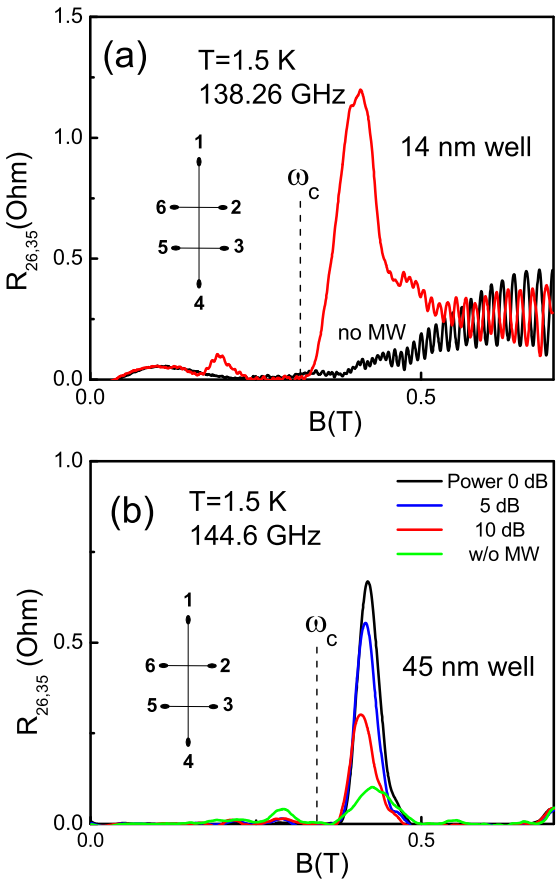

FIG. 2: (Color online) (a) Nonlocal resistance $R_{26,35}$ (I=2,6; V=3,5) under microwave irradiation (143 GHz)in a wide (45 nm) quantum well with decreasing microwave power. (b) Nonlocal resistance $R_{26,35}$ (I=2,6; V=3,5) without (no MW) and under microwave irradiation (144,6 GHz) in a narrow (14 nm) quantum well. Insets show the measurement configuration.

value of $\Delta_{SAS} = 1.40$ meV is extracted from the periodicity of low-field MIS oscillations, see Ref. [13]. Several devices from the same wafers have been studied.

In Fig. 1 we present dark resistance and the observation of a ZRS (marked with an arrow) for 144,6 GHz and at a temperature of 1.5 K in single layer and bilayer Hall bar devices. In the presence of the microwave irradiations MIRO appear in NQW, and one of the minimums develops into ZRS. The resistance of both quantum wells reveals magnetointesubband (MIS) oscillations caused by the periodic modulation of the probability of intersubband transitions by the magnetic field (see Ref. [13]). Note, however, that MIS oscillations in the narrow well are observed at a relatively high magnetic field due to the low second subband density, and are therefore, they are almost unaffected by MW radiation. In contrast, exposing a bilayer system to MW leads to interference of the MIRO and MIS oscillations with enhancement, suppression or inversion of the MIS peak correlated with MW frequency [14]. Moreover, a zero resistance state develops from the MIS maximum [15].

For the same samples with a Hall bar pattern, the nonlocal resistance $R_{NL} = R_{26,35}$ (I=2,6; V=3,5) was also measured. Figure 2 shows $R_{26,35}$ for both types of quantum wells (WQW and NQW) in the presence of microwave irradiation and at different intensities of radiation. Both samples display a prominent peak in nonlocal resistance corresponding to a peak in R_{xx} around $j \approx 3.15/4$. However, examination of figures 1 and 2 reveals a drastic difference between local and nonlocal effects. In particular, the second peak at $B \approx 0.18T$ in local resistance, which has almost the same amplitude as the peak near 0.4 T, vanishes in the nonlocal resistance for WQW. Figure 3 illustrates microwave -induced non-

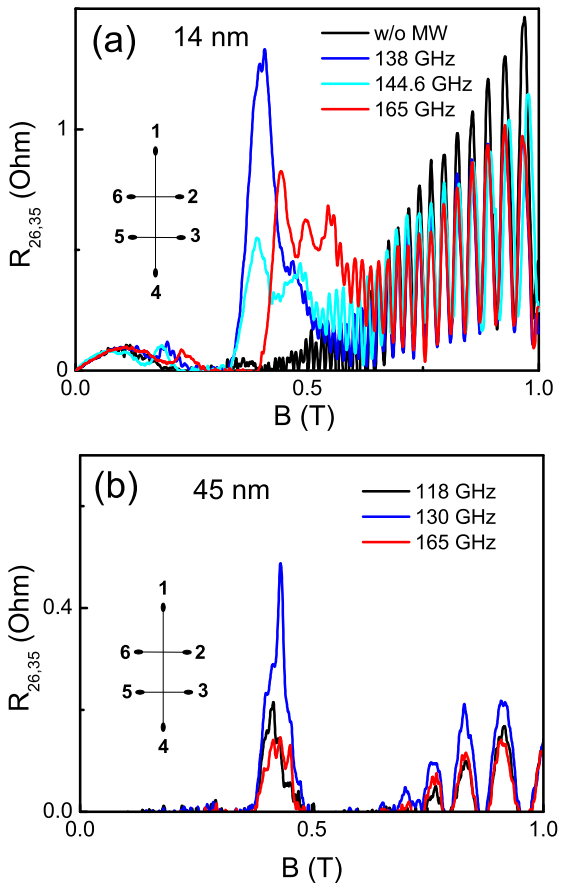

FIG. 3: (Color online) Nonlocal $R_{26,35}$ (I=2,6; V=3,5) resistances for a narrow (a) and wide (b) quantum wells and for different microwave frequencies. Insets show the measurement configuration.

local resistance for three chosen frequencies. One can see only one dominant peak near $B \approx 0.4T$. The magnitude of the peak varies with frequency due to the variation in microwave power. The position of the peak in NQW is correlated with frequency, while, in the bilayer system, peaks developed from combined MIS-MIR oscillations, and therefore, their location depends on subband splitting and is less sensitive to frequency [15].The classical ohmic contribution to the nonlocal effect is given by $R_{NL}^{classical} \approx \rho_{xx} \exp(-\pi L/w)$ for narrow strip geometry where L is the distance between the voltage probes, and w is the strip width [16]. For our geometry we estimate $R_{NL}^{classical}/R_{xx} \approx 3\times10^{-4}$ for a zero magnetic field. In the QHE regime, the nonlocal resistance R_{NL} arises from the suppression of electron scattering between the outermost edge channels and the backscattering of the innermost channel via the bulk states [10, 17, 18]. It appears only when the topmost Landau level is partially occupied, and scattering via bulk states is allowed.

We have also measured the nonlocal response in device B in other geometries and found similar behavior. Note, however, that these samples have less mobility ($0.9\times10^6 cm^2/Vs$), and demonstrate microwave-induced nonequilibrium oscillations of smaller amplitude, without reaching the zero resistance state. These and other measurements described in [12] provide evidence for microwave induced edge state transport in the low magnetic field regime. Nonzero nonlocal resistance implies that the dissipation-less edge state transport persists over macroscopic distances, because the length of the edge channels are determined by the distance between the metallic contacts ($\sim 1mm$), or at least, by the distance between potential probes ($\sim 0.5mm$).

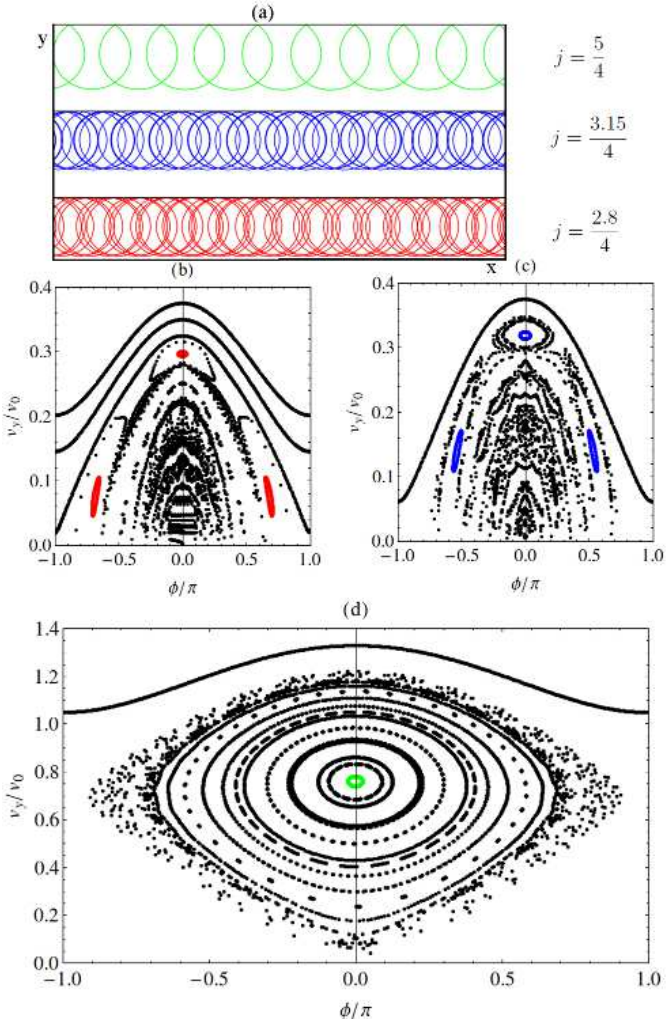

FIG. 4: (Color online) (a) Examples of electron trajectories along the sample edge for several values of $j = 5/4$, 3.15/4, 2.8/4; (b) Poincaré section of for $j = 2.8/4$, (c) $j = 3.15/4$, (d) $j = 5/4$ at y-polarized field with $\varepsilon = 0.02$.

The nonlocal effect described above can be understood within a common framework based on modern nonlinear dynamics. As was indicated in [11] for propagating

edge channels, a microwave field creates a nonlinear resonance well described by the standard map, known as the Chirikov standard map [19]. In our case it is constructed by a Poincarés surface of a section for electrons moving in the vicinity of the sample edge modeled as a specular wall in the presence of the microwave driving field. The details of the model are described in [11]. In order to compare the theory with our experiment, we extend the results of this model to our specific sample parameters and experimental conditions [12]. We are mostly interested in the dynamics of electrons in the vicinity of the ratio $j = 3.15/4$, where the microwave induced peak in the nonlocal response is observed (figs. 2,3). Figure 4a shows electron trajectories in the edge vicinity for different values of the ratio j. One can see that the microwave field strongly modifies the dynamics along the edge. The figures 4 b,c,d show Poincaré sections for the wall model and different values of the magnetic field corresponding to the peak in R_{NL} around $B = 0.42T$ ($j = 3.15/4$), on the high- field side of the peak ($j = 2.8/4$) and on the resistance minima ($j = 5/4$). For $j = 5/4$ Poincaré sections exhibit periodic and quasiperiodic trajectories surrounded by a chaotic sea. For $j = 2.8/4$ and $j = 3.15/4$ Poincaré sections exhibits less stable dynamics, but a periodic component remains present. The existence of the periodic orbits plays a fundamental role in the local and nonlocal resistivity of a 2D gas. The truly dissipationless edge channels may carry the same electrochemical potential μ over a macroscopic distance to the different voltage probes. As a consequence, $\Delta\mu = 0$ which results in vanishing R_{xx} and R_{NL}. If a certain fraction of the edge states are scattered into the bulk, it leads to different local chemical potentials, finite $\Delta\mu$ and resistivity. This situation closely resembles the QHE, when it is possible to treat the edge and bulk conducting pathways separately. This may lead to nonlocal resistivity. For example, in the QHE regime the nonlocal resistance R_{NL} arises from the suppression of electron scattering between the outermost edge channels and backscattering of the innermost channel via the bulk states [10, 17, 18]. It is worth noting that the actual shape of the wall potential is rather parabolic than the hard wall. We have compared nonlinear resonance and Poincaré sections for both potential and found no difference in the dynamics of electrons (for details see [12]).

However, demonstration of the existence of the periodic orbits stabilized by the MW field is not enough to justify the nonlocal response and some further qualitative analysis might be required to compare the magnitude of R_{NL} with calculations using the simple model. In the rest of the paper, we provide a model describing the edge and bulk contribution to local and nonlocal resistance [12]. The mechanism responsible for the observed peak in local and nonlocal magnetoresistance near $j = 3.15/4$ relies on the combination of the edge state and bulk transport contributions, when bulk-edge coupling is taken into account [20]. The bulk electrons and edge modes are consequently described by the local chemical potentials ψ and φ. We can introduce the phenomenological constant g, which represent scattering between modes φ and ψ. The edge state transport can be described by equations for particle density [18, 20], taking into account the scattering between edge modes and the bulk [12]. The model reproduces the experimental values of the local $R_{14,23} \approx 40$ ohm and nonlocal $R_{26,35} \approx 1.2$ ohm resistances with adjustable parameter $g = 0.005\mu m^{-1}$. Note, however, that more precise calculations require exact knowledge of the fractions of electrons channeling along the wall P. Taking into account the total number of the Landau levels near $B \approx 0.42$ T, $N \approx 120$, we may choose $M = P \times N \approx 1 - 3$ and a current carried by edge channels $I \sim Me^2\varphi/h$.

A consensus, based on many experimental studies, including magnetic field, frequency, temperature etc dependencies, now exists concerning the "inelastic" mechanism, which may by now be considered as the dominant contribution to MIRO and ZRS in a high mobility electron system [1]. Moreover, observation of ZRS in Corbino geometry [21] and contactless [22] measurements strongly indicates that microwave induced nonequilibrium effect is the bulk rather than the edge state phenomenon. Our finding may indicate that MIRO and ZRS are a very rich physical phenomenon, which results from a combination of the both bulk and edge state contributions. We believe that ZRS phenomena is somewhat like a quantum Hall effect (although not exactly the same), which can be described as a bulk or/and edge phenomena (see for example [23]). Indeed both descriptions are experimentally supported from measurements: the observation of the nonlocal effects clearly demonstrates edge-state conduction [17], and observation of the charge transfer in Corbino geometry, where edge transport is shunted via concentric contacts, show that the quantum Hall effect as a consequence of pure bulk transport is possible [24].

From our experiment we may conclude that the edge state effect is dominant or comparable with bulk contribution near $\omega/\omega_c \approx 3.15/4$. Note, however, that our result does not explicitly rule out the bulk mechanism near minimum $j = 5/4$ and, therefore, does not contradict with previous investigations.

In conclusion, we have observed a microwave induced nonlocal magnetoresistance peak in the vicinity of the ratio $\omega/\omega_c \approx 3.15/4$. This data offer evidence that, in a low magnetic field, MW induced edge-state transport really extends over a macroscopic distance of $\sim 1mm$. We compare our results to a transport model that takes into account the combination of the edge state and the bulk transport contributions and the backscattering within the bulk-edge coupling.

We thank Z.D.Kvon for helpful discussions. The financial support of this work by FAPESP, CNPq (Brazilian agencies) is acknowledged.

[1] I. A. Dmitriev, A. D. Mirlin, D. G. Polyakov, and M. A. Zudov, Rev.Mod.Phys. B **84**, 1709 (2012).

[2] M. A. Zudov, R. R. Du, J. A. Simmons, and J. L. Reno, Phys. Rev. B **64**, 201311(R) (2001); P. D. Ye, L. W. Engel, D. C. Tsui, J. A. Simmons, J. R. Wendt, G. A. Vawter, and J. L. Reno, Appl. Phys. Lett. **79**, 2193 (2001).

[3] R. G. Mani, J. H. Smet, K. von Klitzing, V. Narayanamurti, W. B. Johnson, and V. Umansky, Nature **420**, 646 (2002); M. A. Zudov, R. R. Du, L. N. Pfeiffer, and K. W. West, Phys. Rev. Lett. **90**, 046807 (2003).

[4] V. I. Ryzhii, Fiz. Tverd. Tela (Leningrad) **11**, 2577 (1969) [Sov. Phys. Solid State **11**, 2078 (1970)]; V. I. Ryzhii, R. A. Suris, and B. S. Shchamkhalova, Fiz. Tekh. Poluprovodn. **20**, 2078 (1986) [Sov. Phys. Semicond. **20**, 1299 (1986)].

[5] A. C. Durst, S. Sachdev, N. Read, and S. M. Girvin, Phys. Rev. Lett **91**, 086803 (2003).

[6] I. A. Dmitriev, M. G. Vavilov, I. L. Aleiner, A. D. Mirlin, and D. G. Polyakov, Phys. Rev. B **71**, 115316 (2005); I. A. Dmitriev, A. D. Mirlin, and D. G. Polyakov, Phys. Rev. B **75**, 245320 (2007).

[7] A.V. Andreev, I. L. Aleiner, and A. J. Millis, Phys. Rev. Lett **91**, 056803 (2003)

[8] J. Inãrrea and G. Platero, Phys. Rev. Lett. **94**, 016806 (2005); J. Inãrrea and G. Platero Phys. Rev. B **84**, 075313 (2011)

[9] S. A. Mikhailov, Phys. Rev. B **83**, 155303 (2011)

[10] M. Büttiker, Phys. Rev. Lett. **57**, 1761 (1986).

[11] A. D. Chepelianskii and D. L. Shepelyansky, Phys. Rev. B **80**, 241308(R) (2009); O. V. Zhirov, A. D. Chepelianskii and D. L. Shepelyansky, Phys. Rev. B **88**, 035410 (2013).

[12] See in Supplemental Material.

[13] N. C. Mamani, G. M. Gusev, T. E. Lamas, A. K. Bakarov, and O. E. Raichev, Phys. Rev. B **77**, 205327 (2008).

[14] S. Wiedmann, G. M. Gusev, O. E. Raichev, T.E.Lamas, A. K. Bakarov, and J. C. Portal, Phys. Rev. B **78**, 121301(R) (2008).

[15] S. Wiedmann, G. M. Gusev, O. E. Raichev, A. K. Bakarov, and J. C. Portal, Phys. Rev. Lett. **105**, 026804 (2010).

[16] L. J. van der Pauw, Philips Tech. Rev. **20**, 220 (1958).

[17] P.L.McEuen, A. Szafer, C.A.Richter, B.W.Alphenaar, J.K.Jain, A.D.Stone, R.G.Wheeler, R.N.Sacks, Phys. Rev. Lett. **64**, 2062, (1990).

[18] V.T.Dolgopolov, A.A.Shashkin, G.M.Gusev , Z.D.Kvon, Pis'ma Zh.Eksp.Teor.Fiz., **58**, 461 (1991) (JETP Lett., **53**, 484 (1991)).

[19] B. V. Chirikov, Phys. Rep. **52**, 263 (1979).

[20] V.T. Dolgopolov, G.V. Kravchenko and A.A. Shashkin, Sol.St.Commun. **78** 999 (1991).

[21] C. L. Yang, M. A. Zudov, T. A. Knuuttila, and R. R. Du, L. N. Pfeiffer and K. W. West, Phys. Rev. Lett. **91**, 096803 (2003).

[22] I. V. Andreev, V. M. Muravev, I. V. Kukushkin, S. Schmult and W. Dietsche, Phys. Rev. B **83**, 121308(R) (2011).

[23] Y-C.Kao, D.-H.Lee, Phys. Rev. B **54**, 16903 (1996).

[24] VT Dolgopolov, AA Shashkin, NB Zhitenev, SI Dorozhkin, von Klitzing K , Phys. Rev. B **46**, 12560 (1992).